Journal of Food Composition and Analysis 125 (2024) 105822

Contents lists available at ScienceDirect

Journal of Food Composition and Analysis

journal homepage: www.elsevier.com/locate/jfca

Ion-exchange purification, nano-HPLC–MS/MS identification and molecular dynamics simulation of novel umami peptides from fermented grain wine (Huangjiu)

Rui Chang [a], Zhilei Zhou [a,b,c], Yong Dong [a], Yue zheng Xu [e], Zhongwei Ji [a,b,c], Shuangping Liu [a,b,c], Min Gong [d,e], Jian Mao [a,b,e,*]

[a] National Engineering Research Center of Cereal Fermentation and Food Biomanufacturing, School of Food Science and Technology, Jiangnan University, Wuxi 214122, Jiangsu, China
[b] Jiangnan University (Shaoxing) Industrial Technology Research Institute, Shaoxing 312000, Zhejiang, China
[c] Jiangsu Provincial Engineering Research Center for Bioactive Product Processing, Jiangnan University, Wuxi 214122, Jiangsu, China
[d] College of Life Sciences, Linyi University, Linyi 276000, Shandong, China
[e] National Engineering Research Center for Huangjiu, Zhejiang Guyuelongshan Shaoxing Wine Co., Ltd., Shaoxing 312000, Zhejiang, China

ARTICLE INFO

Keywords:
Huangjiu
Rice wine
Umami peptides
Molecular docking
Molecular dynamics simulation

ABSTRACT

Huangjiu is a traditional Chinese fermented rice wine with abundant peptides, but the umami peptides are little known due to the wine's complex matrix. Herein, the target umami fraction was enriched with sensory-guided separation coupled with ultrafiltration, ion-exchange, and gel chromatography purification. A total of 1901 peptides were identified from gel F1 fraction with nano-HPLC–MS/MS. Eight novel umami peptides DWDPHGL, VPEPEPH, LTPEPEH, GANQLDPR, FREE, LDFR, QEGW, and RDH were filtered by virtual screening and sensory evaluation. They exhibited thermal stability at 373.15 K and the taste thresholds in water were between 0.29 and 0.65 mmol/L. Among them, RDH was crucial, due to a relatively high dose over threshold (DoT) factor (1.12). Molecular docking results showed that residues ASP147, SER148, ARG151, TYR220, SER276, and ALA302 contributed most to the interaction of peptide and T1R1. Moreover, molecular dynamics simulation and weak interaction analysis suggested the important role of intramolecular forces in peptide thermal stability.

1. Introduction

Umami is an important basic taste in fermented foods, and it can be induced not only by umami molecules such as amino acids and nucleotides, but also peptides. Among them, umami peptides have attracted wide attention due to their functional and flavor characteristics. The umami peptide recognition process involves interacting with the active pocket of the taste receptor T1R1-T1R3, activating the binding domain (Dang et al., 2014). So far, more than 300 umami peptides have been identified, many from fermented soybeans (Zhuang et al., 2016), meat (Dang et al., 2015), and fish (Yang et al., 2022a), while few are derived from fermented grain wines, which also taste of umami and are abundant with peptides. According to some studies, low molecular weight peptides in wines have certain umami potential (Desportes et al., 2001). Sake is a typical Japanese fermented rice wine. Tamami Kiyono et al. identified 19 pyroglutamyl peptides in sake and some could enhance umami taste, such as pyro-Glu-Gln and pyro-Glu-Gly (Kiyono et al., 2013). However, to date, little is known about the umami peptides in other fermented grain wines due to the lack of relevant studies and complex matrix components.

Separation and identification of peptides present in fermented wine are challenging due to the low abundance of target fractions and interference with impurities. Therefore, basic preprocessing before identification is necessary, such as ultrafiltration, precipitation, and desalting. Ultrafiltration is a physical method used for enrichment and preliminary separation. Resin adsorption, gel chromatography, and solid-phase extraction (SPE) are often used for fine purification. For Huangjiu peptide identification, Q-TOF-MS/MS (Han and Xu, 2011) and ESI-MS/MS (Shi et al., 2021) are common methods, but their results are limited in number and accuracy. Unlike these conventional identification

* Corresponding author at: National Engineering Research Center of Cereal Fermentation and Food Biomanufacturing, School of Food Science and Technology, Jiangnan University, Wuxi 214122, Jiangsu, China.
E-mail address: maojian@jiangnan.edu.cn (J. Mao).

https://doi.org/10.1016/j.jfca.2023.105822
Received 8 September 2023; Received in revised form 27 October 2023; Accepted 6 November 2023
Available online 9 November 2023

methods, the newly developed nanoscale high-performance liquid chromatography coupled tandem mass spectrometry (nano-HPLC–MS/MS) has the advantage of high sensitivity, and gives more comprehensive and accurate results. However, the main difficulty associated with it is the screening of target peptides from thousands of peptide results, because synthesis of so many unfiltered peptide sequences one-by-one with subsequent verification of their sensory taste is very expensive and time-consuming. Currently, bioinformatics and artificial intelligence in silico tools have proven to be an efficient method for functional peptides screening. Compared to the traditional filtering process (reliant on liquid-phase separation and mass spectrometry only), molecular docking screening provides more rapid and precise peptide candidate results based on the receptor-ligand structure–activity relationship. Zhang et al. discovered 9 umami peptides by T1R1-T1R3 model docking out of 200 potential umami peptides derived from chicken soup (Zhang et al., 2023a). Xiong et al. also screened 20 umami peptides from a 400 dipeptides library (Xiong et al., 2022). Therefore, promoting this strategy could expand insights into umami peptides in fermented wine.

Huangjiu is a traditional rice wine consumed in China for over 2000 years. It is obtained after fermenting rice with starter wheat koji and JIUYAO. During fermentation, over 600 microorganisms work together to transform raw material proteins into amino acids and peptides, which confer the product's taste and flavors, particularly sweet and umami. The peptide content in Huangjiu ranges from 1.77 to 4.21 g/L (Xie et al., 2016), and over 90% of peptides are within the molecular weight range of 200–3000 Da. Han and Xu (2011) identified over 300 peptides in Huangjiu by UPLC–Q-TOF-MS, but only one peptide (EEE) that may be potentially umami due to identification and isolation limitations. Therefore, umami peptides of Huangjiu warrant further exploration.

The present study employed a sensory-guided fractionation strategy to enrich the umami peptide fractions in Huangjiu. The target fractions were obtained through multistep purification, including crude separation by membrane ultrafiltration, removing the impurities by ion-exchange resin, and refining by gel chromatography. Then, the umami peptides were identified with peptidomics and in silico screening approaches, and quantified by UPLC–TQD-MS. Finally, the relevant mechanism of screened peptides were explored through molecular docking and dynamics simulation.

2. Materials and methods

2.1. Materials and reagents

A mechanical craft was employed to bring 20 L of low-sugar Huangjiu from a famous winery in Shaoxing, China, then stored at –20 ℃. Analytical-grade sodium hydroxide, hydrochloric acid, phenol, sulfuric acid, glucose, Folin phenol, and gallic acid were purchased from Sinopharm Chemical Reagent Co. Ltd., Shanghai, China. Food-grade sodium chloride, citric acid, sucrose, quinine, glutathione, and monosodium glutamate (MSG) were purchased from Gino Biotech Co. Ltd., Zhengzhou, China. Food-grade ammonium hydroxide was provided kindly by Surong Auxiliary Co. Ltd., Taixing, China.

2.2. Separation and purification of peptides in Huangjiu

The method of separation and purification of peptides in Huangjiu was based on a sake study with some modification (Kiyono et al., 2013). The molecular weight of the purification fractions was measured using the Wen et al. method (Wen et al., 2022).

2.2.1. Ultrafiltration

Raw Huangjiu samples were centrifuged at 8000 rpm for 20 min at 4 °C, and the supernatant was filtered through a 0.22-μm filter membrane to remove crude impurities. After the ultrafiltration, the obtained peptide fractions with molecular weight less than 3000 Da were concentrated by rotary evaporator (50 °C, 0.098 MPa vacuum) and then freeze-dried. The content of total peptide, total sugar, and total polyphenol in these fractions were measured (Yang et al., 2022b), using the Pierce BCA assay kit (Thermo Fisher Scientific, Waltham, MA), sulfuric acid phenol, and Folin phenol reagent, respectively. The peptide content (g/100 g) was calculated as its percentage in the sum of the three aforementioned components.

2.2.2. Resin purification

For resin pretreatment, 100 g of strong acid cation exchange resin Amberlite 120 IRB (Bailing Biology Corp., Shanghai, China) were soaked with 95% ethanol for full swelling. Then, ethanol was removed and the resin converted into H^+ form through soaking with 1 mol/L HCl for 2 h followed by washing with deionized water, until the effluent reached pH 6. The processed resin was packaged into a glass column (Φ2.6 × 30 cm). Next, 20 mL of the Huangjiu ultrafiltration sample (with molecular weight less than 3000 Da, peptide concentration 25 mg/mL, pH adjusted to 4) were carefully loaded into the column at a flow rate of 5 mL/min, followed by static adsorption for 6 h at 4 °C. In the elution step, 500 mL deionized water were added to the column at a rate of 5 mL/min to remove the incomplete bound peptides and soluble sugars, followed by 800 mL 1 mol/L ammonia hydroxide to recover the peptides. The eluent was then subjected to rotary evaporation at 50 °C for the removal of ammonia, and, freeze-dried and stored at –20 ℃.

2.2.3. Gel chromatography

The resin-purified crude peptide powder was dissolved in water at a concentration of 10 mg/mL, and the solution was then filtered through a 0.45 μm membrane. Sample (5 mL) was loaded onto a Sephadex G15 gel column (Φ1.2 × 100 cm; Solarbio Corp., Beijing, China) for fractionation. The target fraction was eluted using pure water at a flow rate of 1 mL/min. The absorption peak of the peptides in the eluent was detected at 220 nm. Eluent fractions with similar absorption peaks were collected partial, then freeze-dried, and stored at –20 ℃.

2.3. Identification of peptides using nano-HPLC–MS/MS

The fraction with the highest umami taste intensity was identified by nano-HPLC–MS/MS (Zan et al., 2023). The samples were desalted with Pierce C18 Spin Tips and then re-dissolved in solvent A (0.1% formic acid in water), followed by analysis using Q-Exactive Plus coupled to an EASY-nanoLC 1200 system (Thermo Fisher Scientific, Waltham, MA). The sample (6 μL) was loaded onto an analytical column of 25 cm with 75 μm inner diameter and 1.9 μm resin (Dr Maisch) at a flow rate of 300 nL/min, then separated using 2% buffer B (80% ACN with 0.1% FA) with a 60 min gradient starting, stepwise increase to 35% within 47 min and then to 100% in 1 min, and maintained for 12 min. The column temperature was 40 °C and the electrospray voltage was set to 2 kV. The mass spectrometer was run in data-dependent acquisition (DDA) mode. The full-scan MS spectra (m/z 200–1800) survey was conducted with a resolution of 7×10^4. The automatic gain control (AGC) target was 3×10^6, and the maximum injection time was 50 ms. Next, the precursor ions were selected in the collision cell for fragmentation by higher-energy collision dissociation (HCD). The MS/MS resolution was set to 1.75×10^4, and the AGC target was 1×10^5, the maximum injection time was 45 ms, and the dynamic exclusion was 30 s. Tandem mass spectra were processed by PEAKS Studio version 10.6 (Bioinformatics Solutions Inc., Waterloo, Canada), including de novo sequencing and database match for short peptides (length 2–4) and medium-length peptides (larger than 4), respectively. For database match, proteomes of *Oryza sativa* subsp. Japonica, *Triticum aestivum*, and *Saccharomyces cerevisiae* (strain ATCC 204508/S288c) were acquired from the UniProt database. No digestion enzyme was selected.

2.4. Virtual screening and molecular docking

The identified peptides with a –10 lgP and confidence level greater than 20 were selected for further analysis. Next, based on the length of most of the reported umami peptides, the peptides with a maximum sequence length of 10 amino acids were selected. Each selected peptide was evaluated for its umami potential using the machine learning models and online tools BIOPEP-UWM (Minkiewicz et al., 2019); https://biochemia.uwm.edu.pl/biopep-uwm/), UMPred-FRL (Charoenkwan et al., 2021); http://pmlabstack.pythonanywhere.com/UMPred-FRL), and Umami_YYDS (Cui et al., 2023); http://www.tastepeptides-meta.com). The filtered peptides were then screened via docking with the taste receptors.

2.4.1. Taste receptor model preparation

When the sequence similarity between the target and the template protein was over 30%, the model established by homology modeling had a confidence level of 80% or greater. For the umami receptor, the fish sweet taste receptor (PDB: 5×2M) was used as the template, owing to its high homology (37.45%) with the human hT1R1-T1R3 protein (Liu et al., 2019), which is slightly better than the homology percentage (23.88%) of template 1EWK (Li et al., 2020). For sweet receptor T1R2-T1R3, 5×2M was also applied as the template protein. The protein sequences of the human umami taste receptors Q7RTX1 (TAS1R1), Q8TE23 (TAS1R2), and Q7RTX0 (TAS1R3) were retrieved from the UniProt database, and homology modeling was performed by the SIWSS-MODEL server. The model with the highest GMQE score was adopted as the candidate model. The ERRAT, VERIFY 3D, and PROCHECK tools were then employed to evaluate the rationality of the modeled structure.

Bitter receptors including TAS2R4, TAS2R14, TAS2R16, TAS2R38, TAS2R39, and TAS2R46 were obtained from BitterDB (https://bitterdb.agri.huji.ac.il/dbbitter.php). For kokumi taste receptor, calcium-sensitive protein (PDB: 5K5S) was used.

2.4.2. Molecular docking

The peptide structure was drawn by ChemDraw and optimized under the MMFF94 force field. The active site of the modeled umami receptor was determined through protein alignment by the 5×2M ligand. The docking position included the umami receptor T1R3 site (x, y, z = 51.31, 40.38, 12.71) and the T1R1 site (x, y, z = 39.05, 25.33, 40.88). Others also determined with receptor cavity positions, sweet receptor T1R3 (x, y, z = 51.09, 39.56, 9.33) and T1R2 (x, y, z = 47.29, 27.84, 36.46), kokumi 5K5S (x, y, z = 178.25, 47.86, 167.67), as well as bitter TAS2R4 (x, y, z = 0.95, 0.81, 8.38), TAS2R14 (x, y, z = 1.19, 2.03, 11.99), TAS2R16 (x, y, z = 0.79, 3.70, 12.39), TAS2R38 (x, y, z = 3.90, 1.43, 12.30), TAS2R39 (x, y, z = 1.09, 1.74, 12.59), TAS2R46 (x, y, z = 140.16, 136.74, 102.48). All of the active cavity sizes were set to 25 × 25 × 25 Å. The docking was performed by AutoDock Vina 1.1.2. Docking for medium-length peptides (larger than 4) was performed with T1R1-T1R3 only, and all taste receptors were used for short peptides (2−4), as they were easily bound to multiple taste receptors with a relatively small molecular volume.

2.5. Solid-phase synthesis of peptides

The candidate umami peptides screened from molecular docking were solid-phase synthesized by Shanghai Gill Biochemical Co., Ltd (Shanghai, China) with purity not lower than 95%.

2.6. Sensory evaluation and quantification

2.6.1. Taste descriptive analysis

The method reported by Chen and Zhuang was adopted with slight modifications (Chen et al., 2021; Zhuang et al., 2016). Ten sensory evaluation panelists (five men and five women, aged 25–30), who had no history of known taste impairment/disorders, were recruited and trained. All panelists gave their informed consent before every sensory session. The sensory evaluation was conducted inside a room at 24 °C, in accordance with ISO-8586–1, 2012. The standard taste solutions used for sour, sweet, bitter, salty, umami, and kokumi containing 0.08% citric acid, 1% sucrose, 0.08% quinine, 0.35% sodium chloride, 0.35% monosodium glutamate (MSG), and 0.15% glutathione, respectively. The Huangjiu fractions containing peptides less than 3000 Da, which had been purified using resin and gel, were dissolved in water at a concentration of 10 mg/mL. The panel members sipped each sample (4 mL) for 10 s prior to spitting it out. After the evaluation of one sample, the members washed their mouths with pure water and rested for 3 min to eliminate fatigue. All samples were scored on a sensory scale with a score range of 0–9 points, with 0 representing pure water and 5 representing standard solutions. The taste characteristics and intensity scores of all panelists were averaged to obtain the corresponding final values.

2.6.2. Taste dilution analysis (TDA)

The aqueous solution of lyophilized fractions (10 mg/mL) was gradually diluted with deionized water at 1:1 (*v/v*) and then used for evaluation (Zhang et al., 2022). In the evaluation, the taste dilution (TD) values were recorded as the degree of dilution when distinguished the umami taste difference between the fraction with two cups of water. The TD values of all panelists were averaged to obtain the final results. The samples with the highest TD value and umami taste were selected for subsequent analysis.

2.6.3. The taste characteristics of synthetic peptides

The peptide solution was prepared in pure water at a concentration of 2 mg/mL and then used for the descriptive sensory evaluation. The samples were tasted twice by the sensory panelists and intensity scores were given in the range of 0–5. In the thermal stability test, the peptide solutions (2 mg/mL) in glass tubes were boiled at 100 °C (373.15 K) for 30 min and then cooled to 25 °C (298.15 K) for the next sensory evaluation.

2.6.4. The taste threshold of synthetic peptides

The method reported by Liu et al. (2020) was adopted. The synthetic peptides were diluted with water at 1:1 (*v/v*), and evaluation startED with concentration step increases. The threshold concentration range was preliminarily determined based on the results of the sensory descriptive trial. In order to prevent fatigue, the tests commenced at concentration levels that were two dilution steps below the individual thresholds. Namely, 0.0625 mg/mL was used as the initial evaluation concentration, followed by 0.125, 0.25, 0.5, 1, and 2 mg/mL. The individual thresholds of all the panelists were averaged to determine the overall taste threshold.

2.6.5. Umami enhancement of synthetic peptides

The peptides were dissolved in 0.35% MSG solutions to final concentration 1 mg/mL and then subjected to the umami enhancement evaluation, in which the umami intensity score range was 0–9. For the thresholds of umami enhancing, the comparative taste dilution analysis was adopted (Zhang et al., 2023a).

2.6.6. Quantification of umami peptides

The concentration of sensory verified umami peptides in Huangjiu was quantified through an ACQUITY UPLC–TQD-MS system (Waters Corporation, Milford, MA, USA) under multiple-reaction-monitoring (MRM) mode, refer to Zhang et al. method with modification (Zhang et al., 2021). The five-point external standard peptide solutions calibration curves was prepared for quantitative processes. Under ESI source positive mode, 10 μL of each peptide standard solution (0.2 mg/mL) was injected for automatically optimizing parameters, including precursor ion (*m/z*), product ions (*m/z*), cone voltage (V), and collision energy (eV). The capillary voltage of 2 kV, desolvation

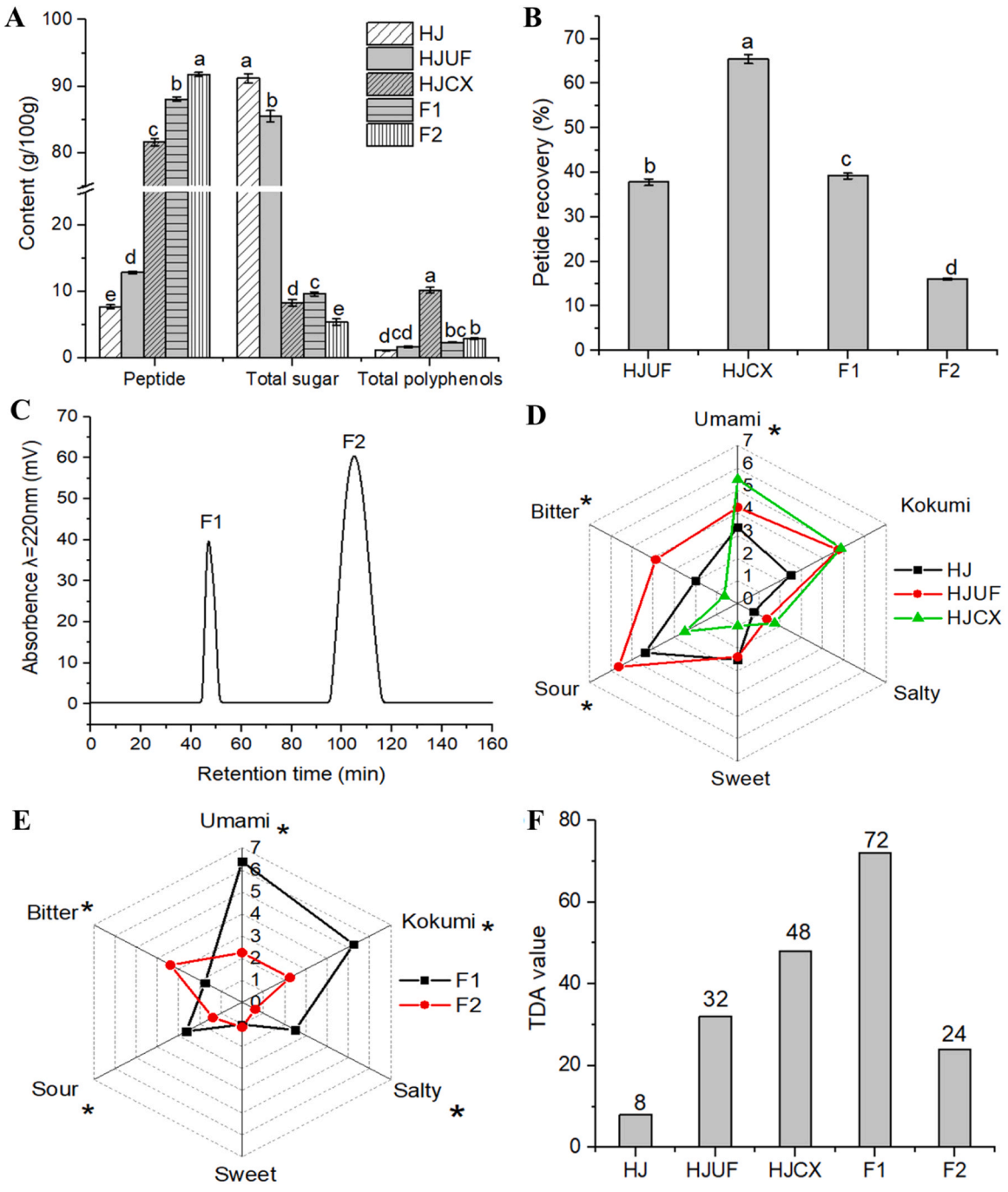

Fig. 1. Sensory characteristics of separated Huangjiu umami peptide fractions (Fig. A: peptide content, Fig. B: recovery rate, Fig. C: gel chromatography ultraviolet response curve, Fig. D and Fig. E: sensory intensity of peptide fractions, Fig. F: umami taste dilution values of fractions). Note, the asterisks in sensory radar chart represent significant differences ($p < 0.05$).

temperature of 400 ℃, and desolvation gas flow 800 L/h was applied. The separation was performed by a C18 column (ACQUITY UPLC BEN C18 Column; 2.1 × 100 mm, 1.7 μm), with mobile phases 0.1% (*v/v*) formic acid in water as solvent A, and 100% ACN as solvent B, flow rate 0.2 mL/min. Huangjiu samples ($n = 3$) were analyzed using the optimized parameters above. MassLynx software (Version 4.0) was used for data processing.

2.7. Molecular dynamic simulation to T1R1 receptor

The medium-length (larger than 4) umami peptide with highest intensity was selected to construct a complex with T1R1 and conducted molecular dynamic in water box (9.8 ×9.8 ×9.8 Å). All simulations were performed using Gromacs software (version 2022). After minimization with the conjugate gradient, 20 ns of NPT restraint pre-equilibrium was simulated under the Amber99SB-Ildn force field, followed by 100 ns of production simulation to obtain the trajectory. In the pre-equilibrium step, the system was heated by the Berendsen temperature coupling method. In the production simulation, the simulation step was 0.002 ps, and the temperature and pressure were controlled using V-rescale and Parrinello-Rahman, respectively. The coulomb interaction was handled using the PME (particle mesh Ewald) method with a Van der Waals threshold of 1.0 nm. The trajectory analysis including RMSD values, hydrogen bond counts, Lennard-Jones short range potential, free energy

landscape and MMPBSA energy decomposition, were finished by gmx tools. Moreover, the averaged independent gradient model (aIGM) was used for the intermolecular interactions forces between peptide and receptor T1R1 (Lu and Chen, 2023).

2.8. Thermal stability mechanism exploration

The same parameters were used for the Peptide-T1R1 complex simulation, and the backbone stability of four medium-length (larger than 4) peptides was investigated at different temperatures (373.15 K and 298.15 K). Every peptide chain was filled with the TIP3P water model in a periodic cubic box (4.2 ×4.2 ×4.2 Å). The RMSD displacement value and the hydrogen bond counts were applied to evaluate the thermal stability.

The density functional theory calculations were performed to obtain intramolecular structural features of the peptides. The peptide structure was optimized at the B3LYP/TZVP level using the D3 dispersion correction by ORCA software (version 5.03), and also obtained the wave functions files. The IRI analysis has been applied widely to evaluate the chemical bonds and weak molecular interactions of organic molecules and is based on the electron density ρ supported by wave function files (Lu and Chen, 2021). In the present study, the IRI weak interaction analysis was performed by the Multiwfn 3.7 (Lu and Chen, 2012) program, followed by visualization of the results using the VMD program; the grid point density of the cube file was 0.15 bohr.

2.9. Data analysis

All assays were performed in triplicate. The data analysis of variance (ANOVA) and Duncan's test were performed on pairs using SPSS (version 23.0, SPSS Inc., Chicago, IL). Results were considered statistically significant at $p < 0.05$. Origin software was employed for data visualization (Pro 2016; OriginLab Corp., Northampton, MA). The peptide–receptor docking mode was performed using VMD, and the residues binding was visualized using Ligplot+; the interaction bonds heatmap was drawn by Hiplot (https://hiplot.com.cn/).

3. Results and discussion

3.1. Sensory-guided separation of Huangjiu peptides fraction

Considering that molecular weights of most reported umami peptides are below 3000 Da (Cui et al., 2023), ultrafiltration treatment with 3000 Da cut-off was first performed to remove the major impurities (proteins, polysaccharides) in Huangjiu (Zhou et al., 2021). The Huangjiu sample (HJ) had peptide, total sugar, and total phenol content of 4.25 ± 0.05, 50.40 ± 0.73, and 0.62 ± 0.03 g/L, respectively. In order to make the purification process convenient, the amino acids and nucleotides were not measured, as they were not major impurities compared to soluble sugars. The peptides content and taste intensity changes after ultrafiltration are shown in Fig. 1A and D. From the results, the HJUF fraction (less than 3000 Da) exhibited a 67.70% increase of peptide content (12.88 ± 0.19 g/100 g) relative to initial HJ (7.68 ± 0.36 g/100 g), and also enhanced taste scores of umami (4.25), kokumi, sour, and bitter (Fig. 1D). Considering the high total sugar (85.48 g/100 g) in the HJUF fraction, the next purification was performed by cation exchange resins. Strong acid cationic resins performed well in the discovery of umami beef octapeptide (Yamasaki and Maekawa, 1978) and sake pyroglutamyl peptides (Kiyono et al., 2013). According to the results of the present study (Fig. 1A), the resin-purified fractions (HJCX) exhibited a peptide purity of 81.58 g/100 g, which represented a peptide enrichment effect 6.37 times that of HJUF. The sugar content in HJCX had decreased to 8.26 g/100 g. The results of the sensory analysis (Fig. 1D) indicated that the HJCX fraction exhibited the highest intensity of umami taste (score 5.5), followed by kokumi, and a little astringency, due to the presence of certain phenols (10.15 g/100 g). The peptide molecular weight of fraction HJCX was mostly below 1500 Da (92.33% of total peptides). HJCX was subjected to further separation by Sephadex-G15 gel, with a working range of 100–1500 Da, resulting in two fractions F1 and F2 (Fig. 1C). The ultraviolet detector response curves indicated that the gel separation was effective. Although the peptide purity of the F1 fraction (88.05 ± 0.28 g/100 g) was lower than F2 fraction (91.76 ± 0.32 g/100 g), its umami intensity (score 6.37) was much higher than F2 (score 2.25), and also the umami dilution values was the highest in all fractions (Fig. 1E and F). In addition, the peptide recovery rate of the F1 fraction (39.22%) was 2.43 times that of the F2 fraction (Fig. 1B). The ratio of the molecular weight larger than 500 Da of F1 fraction (4.65%) was almost four times to F2 (Table S1). Meanwhile, F1 fraction has more (38.98%) short length peptides (200–500 Da) than F2 (17.06%). This indicated that F1 fraction may contain more target umami peptides. Therefore, the gel-separated F1 fraction was accepted as the target fraction for peptides identification.

3.2. Umami peptides virtual screening

3.2.1. Umami peptides prediction

In the F1 fraction, 1901 peptide sequences were identified, and 1739 peptides with length not above ten amino acids were selected for machine learning-based prediction (BIOPEPE, UMPred-FRL, and UmaniDB). Thereafter, 23 potential umami peptides with medium length (larger than 4), and 19 short peptides (length 2–4) were used in the subsequent docking analysis, and the results are listed in Tables S2–S4.

3.2.2. Homology model building

The crystal structure of human hT1R1-T1R3 remains unknown, but the homology modeling methods are widely employed to construct a reasonable structure based on the similarity with template protein sequences (Spaggiari et al., 2020). The structural model of T1R1-T1R3 was constructed by SWISS-MODEL (Fig. S1A). The values of QMEAN (qualitative model energy analysis) and GMQE (global model quality estimate) were used for model selection; the higher values refer to a better model. QMEAN is a scoring function that assesses the geometrical properties of the protein structure. GMQE combines the properties from the target–template alignment and the template structure. In this study, the build model was obtained with GMQE score 0.38, QMEAN score 0.68 ± 0.05, and overall quality score 89.01. The further non-bonded atom interactions validation was applied with SAVES server, and the results revealed an ERRAT value of 89.01, which was within the rejection limit (below 95%). Moreover, the VERIFY 3D analysis indicated that 90.29% of residues had an average score not lower than 0.2 (Fig. S1C and D), indicating good sequence compatibility of the model. This was in line with the results reported by Liang et al., who selected metabotropic glutamate receptors (PDB: 6N51) as the template (Liang et al., 2022). Since the conformation of protein backbone was related to the dihedral angles of α-carbon atoms, stereo-chemical characteristics were analyzed by Ramachandran maps. The results revealed that 90.05% of the amino acid residues were distributed in the best acceptable region, with an allowed region of 99.5%. This demonstrated that the model structure was reasonable (Fig. S1B). The red regions indicate the preferred regions, the yellow regions indicate the allowed regions, the light yellow regions indicate the roughly-allowed regions and the white regions indicate the regions not allowed. Overall, it was demonstrated that the constructed model could be used for the subsequent docking simulation.

3.2.3. Molecular docking screening

The umami peptides exhibit their characteristic taste as interacting with the active residues of the T1R1-T1R3 ligand-binding domain. Both T1R1 and T1R3 contain a receptor cavity to which peptides could bind, although in vitro experiments confirmed the T1R1 domain was the main one. However, certain studies have also reported that the T1R3 domain also binds the umami peptide firmly. For instance, Li et al. proved that

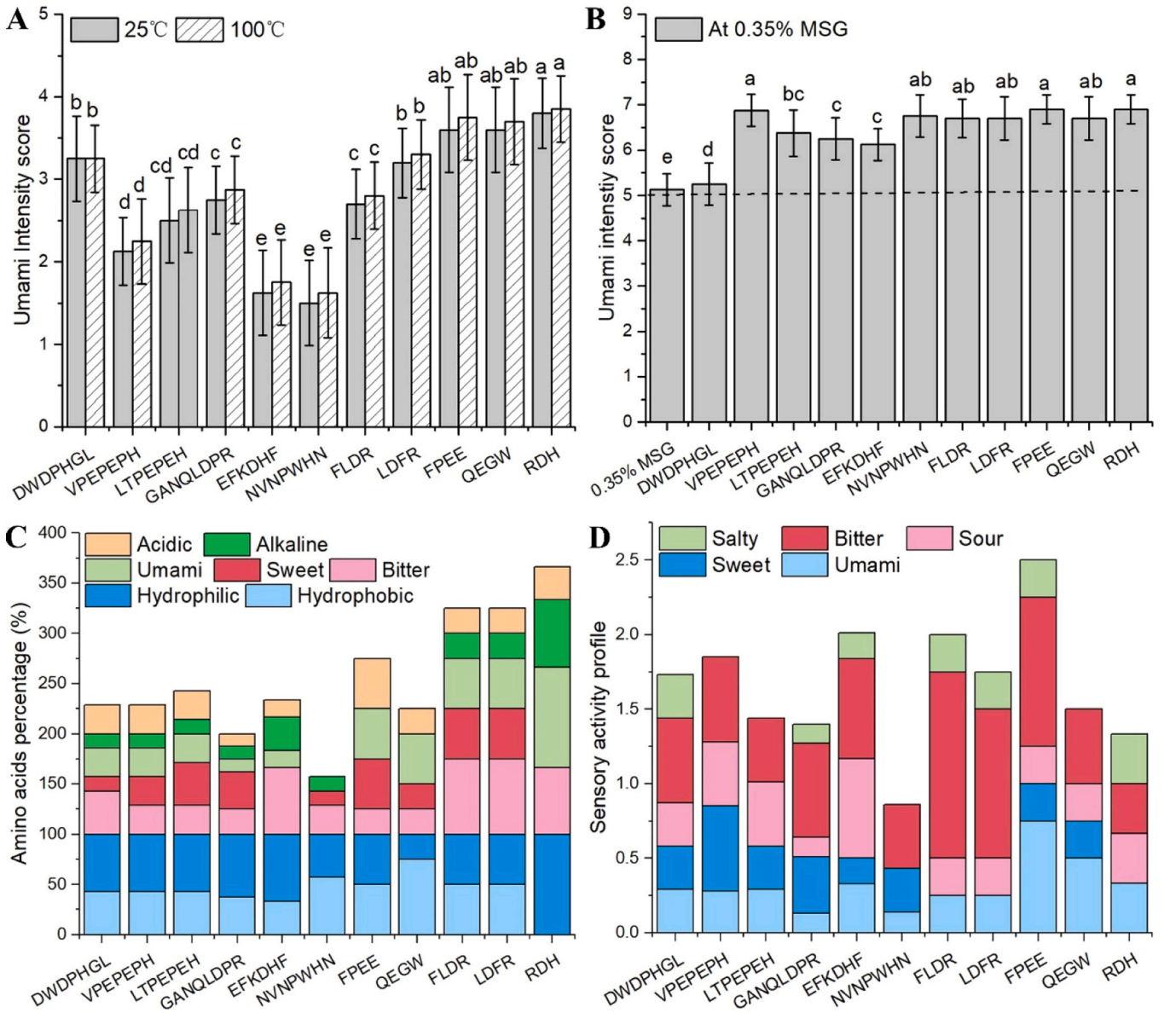

Fig. 2. Sensory and sequence features of synthetic peptides (Fig. A: Umami intensity at different temperature, Fig. B: Umami-enhancing effect, Fig. C: Amino acid composition, Fig. D: Taste activity profile). The different letters in Fig. A and Fig. B represent significant differences ($p < 0.05$).

the umami long-chain 8–9 peptides was harder to bind with T1R1 than T1R3 domain when at docking region size 16 Å (Li et al., 2023). Interestingly, when using a larger box (~20 Å), other studies (Zhang et al., 2023a, 2022) demonstrated that umami peptides tend to bind with T1R1 mostly. Therefore, in the present study, the binding energies of the identified peptides with T1R1 and T1R3 were both calculated. For short peptides, the sweet, bitter and kokumi taste receptors were also considered, to better understand selective interaction during taste recognition on tongue surface cells.

After virtual screening by umami potential prediction tools, 43 peptides were used for the next docking filter. The results are shown in Tables S2 and S3. To select potential umami peptides more effectively, some low-abundance medium-length peptides were omitted from docking results, as they may contribute less to the overall taste; this reduces the synthesis cost.

Finally, six novel candidate medium-length umami peptides were selected with the criteria of abundance area larger than 1×10^6 and binding energy less than −8.6 kcal/mol. These were EFKDHF, DWDPHGL, NVNPWHN, GANQLDPR, LTPEPEH, and VPEPEPH, which were derived from the Japonica rice 1,4-α-glucan-branching enzyme (1,4-alpha-glucan-branching enzyme), Japonica rice chloroplast protein TOC75 (Protein TOC75, Chloroplastic), Japonica rice B4 glutelin, Japonica rice A2-type glutelin, wheat protein kinase domain (uncharacterized protein), and Japonica two-component response regulator ORR3 (two-component response regulator ORR3), respectively. These protein accession annotations indicated the candidate umami peptides were mostly derived from rice or wheat, thereby demonstrating the positive role of raw grain for peptides release in Huangjiu.

For short peptides (2−4), binding energy heatmap results revealed that they formed interaction with multiple taste receptors (Fig. S2). According to the binding preference, we excluded the peptides that tended to bind to bitter receptors rather than the umami receptor. The more blue areas, the easier it is to interact with the corresponding taste receptors (Fig. S2). The screened peptides RDH, FLDR, LDFR, FREE, and QEGW were candidate umami peptides for the next analysis. Because short peptides can be derived from various cleavage processes of many proteins, making the protein source difficult to elucidate accurately, they are not discussed here.

Table 1
Taste threshold of target synthetic peptides.

Peptides	Sensory description	Taste threshold (mmol/L)		Mass (Da)
		in water	in MSG	
DWDPHGL	Umami, sweet, sour	0.39 ± 0.09^{de}	0.48 ± 0.15^{b}	838.36
VPEPEPH	Weak umami, weak sour	0.52 ± 0.16^{cd}	0.28 ± 0.05^{e}	803.38
LTPEPEH	Weak umami, strong sour	0.57 ± 0.21^{c}	0.45 ± 0.16^{bc}	821.39
GANQLDPR	Weak umami, weak kokumi	0.65 ± 0.20^{bc}	0.43 ± 0.15^{bc}	869.43
EFKDHF	Slight umami, sour	0.80 ± 0.17^{b}	0.46 ± 0.16^{bc}	821.37
NVNPWHN	Slight umami, kokumi	0.99 ± 0.13^{a}	0.36 ± 0.13^{cd}	879.39
FLDR	Weak umami, bitter	0.54 ± 0.19^{cd}	0.27 ± 0.10^{e}	549.29
LDFR	Umami, weak bitter	0.39 ± 0.11^{de}	0.41 ± 0.10^{bc}	549.29
FPEE	Umami, sour	0.38 ± 0.12^{de}	0.26 ± 0.07^{e}	520.22
QEGW	Umami, bitter	0.29 ± 0.10^{e}	0.31 ± 0.12^{cd}	518.21
RDH	Umami, weak sour	0.32 ± 0.10^{de}	0.52 ± 0.12^{a}	426.20

* Different letters in the same column represent significant differences ($p < 0.05$).

3.3. Umami characteristics of the target synthetic peptides

Further sensory analysis of the synthetic peptides demonstrated that mostly short peptides (length 2–4) FREE, LDFR, QEGW, and RDH expressed a stronger umami taste in water compared to medium-length DWDPHGL, VPEPEPH, LTPEPEH, and GANQLDPR. In contrast, umami of peptides EFKDHF, NVNPWHN, and FLDR was weaker (Fig. 2A). Among the medium-length peptides, DWDPHGL exhibited the highest umami taste intensity (3.25), followed by GANQLDPR (2.75). In short peptides, RDH was the most umami peptide, next to FPEE and QEGW. Compared to 298.15 K (25 ℃), the taste intensity of all peptides was not changed significantly after handling at 373.15 K (100 ℃), showing that they have thermal stability (Fig. 2A). The taste recognition thresholds of the above eight umami peptides in water ranged from 0.29 ± 0.10–0.65 ± 0.20 mmol/L (Table 1), and the threshold values were lower than that of MSG (1.6 mmol/L), marmoreus hydrolysate umami peptide EGTAG (8.26 mmol/L) (Chang et al., 2023), and soybean paste umami peptide ALDELGT (1.84 mmol/L) (Zhao et al., 2022). Although the umami taste of NVNPWHN was weak, it exhibited obviously kokumi in water and an umami enhancement effect in the case of 0.35% MSG (intensity score 6.75), and the threshold in 0.35% MSG was 0.36 ± 0.13 mmol/L. Moreover, in 0.35% MSG, all short peptides as well as VPEPEPH and LTPEPEH increased umami taste to intensity values from 6.37 to 6.9 (Fig. 2B); VPEPEPH and FLDR had the lowest threshold values of 0.28 ± 0.05 and 0.27 ± 0.10 mmol/L, respectively.

Quantitative analysis shows that the concentrations of most umami peptides in Huangjiu were much lower than their taste threshold values (from 0.43 to 22.73 mg/L), except for RDH, which was 154 ± 0.36 mg/

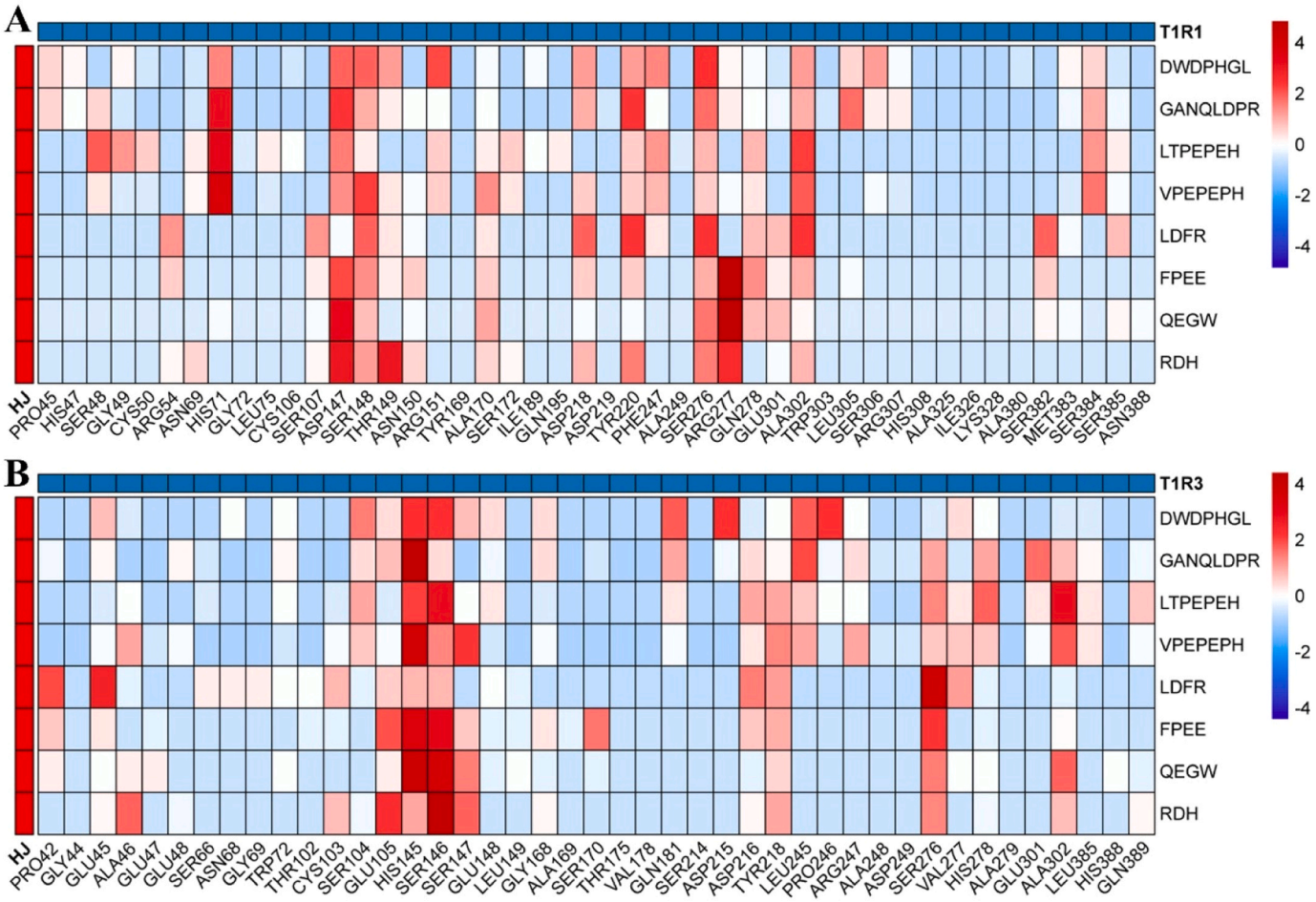

Fig. 3. The interaction bonds heatmap between umami peptides and umami T1R1-T1R3 receptor (Fig. A for T1R1 and Fig. B for T1R3). Note, the scale bar with more red color means the higher frequency of contact.

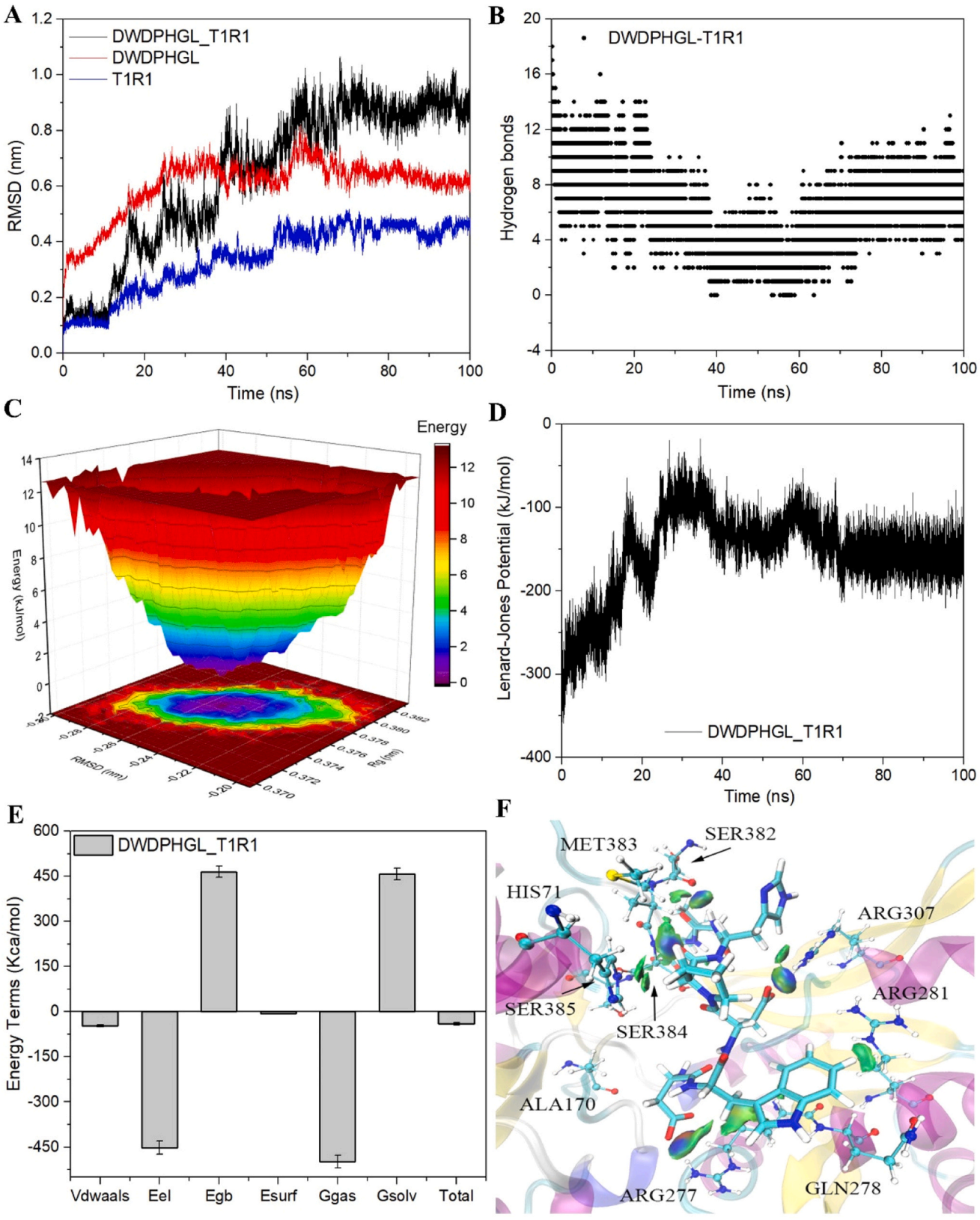

Fig. 4. The molecular dynamic simulation trajectory analysis of DWDPHGL-T1R1 complex (Figs A, B, C, D, E, F represent RMSD values, hydrogen bond counts, free energy landscape, Lennard-Jones short range potential, total energy decomposition and averaged independent gradient model, respectively). Note, The green and blue isosurfaces in Fig. F represent the van der Waals force and hydrogen bond interaction, respectively.

L. This was similar to the results of Zhang et al. (2021). They quantified 13 umami peptides (length more than 4) derived from *Ruditapes philippinarum*, and found that most of them were at concentrations much lower than their taste threshold values. For example, the amount of umami peptide RVSNCAA in *Ruditapes philippinarum* was 0.03 mg/mL, compared with its threshold value of 0.24 mg/mL (Zhang et al., 2021). Among them, the dose over threshold (DoT) value of the highest umami intensity peptide KSAEN was 1.35. In this study, the DoT of RDH was 1.12, indicating that RDH may be the crucial umami taste component in Huangjiu.

In general, the difference in taste of peptides is due to hydrophobicity, amino acid character, and residue during solid-phase synthesis. In order to explore the sequence characteristics of umami peptide, the percentage of amino acid composition and taste profile were determined. As depicted in Fig. 2C, bitter, hydrophobic, and alkaline amino acids were present in all the peptides investigated. All eight umami peptides had a certain proportion of umami, sweet and acidic amino acids, except for RDH, and weak umami peptide NVNPWHN also lacked umami amino acids. This indicated that sweet, umami, and bitter amino acids were critical to peptide taste. According to the Shen et al. study, the content of the bitter taste amino acids (P, L, A) and sweet (A) and umami (E) was over 300 mg/L, accounting for 50.4% of the total amino acid content (Shen et al., 2010). Meanwhile, the C-terminal amino acids of the medium-length umami peptides DWDPHGL, LTPEPEH, VPEPEPH, and GANQLDPR were basic or hydrophobic residues (L, H, R). This was similar to a previous umami peptide analysis, which revealed that for long-chain (5−10) peptides, basic (R, H, K) and hydrophobic amino acids (A, V, L, I, F, P) at the C-terminus contributed significantly to the umami taste (Wang et al., 2022).

Apart from taste-related amino acids, sensory active fragments are also beneficial to umami peptide taste. The results of the BIOPEP sensory profile analysis revealed that all the identified peptides had at least one umami fragment among D, E, or NP, and the sensory evaluation confirmed the umami taste (Fig. 2D). Moreover, all peptides had a higher bitter activity compared to other tastes, attributed to abundant bitter fragments F, K, V, P, W, L, R, along with EF, PR, LD, PR, and GL. However, no significant bitterness was perceived in any medium-length peptide, which could be related to the bitter inhibitory effect of the umami fragment (Kim et al., 2015). In addition, all peptides that contained the sour fragment tasted a little sour, and the effect of the sour fragment on umami peptide taste can be negative. For instance, EFKDHF had the highest umami activity value (0.38) in medium-length peptides, while the sensory intensity (1.63) was not the best. This could be due to the EF sour dipeptide fragment at the N terminal, which inhibited umami taste, as VP did in VPEPEPH; similarly for short peptide FPEE, for which umami activity value was up to 0.75, but was not the most umami. In general, the sweet fragment exerts significant positive effects on umami. Therefore, although GANQLDPR exhibited the lowest umami activity value (0.13), it tasted umami in the sensory evaluation. This could be attributed to the umami-increasing effects of the sweet fragments G, A, and Q with umami amino acid D (Wang et al., 2022).

3.4. Umami peptides and receptor T1R1-T1R3 docking analysis

In the 2D binding mode diagram in Figs. S3 and S4, green lines represent hydrogen bond forces and arcuate residues for hydrophobic interactions. The heatmap of the contact bond numbers between the eight umami peptides and the receptor T1R1-T1R3 key residues is depicted in Fig. 3. The scale bar with a more red color means a higher frequency of contact. According to the docking results in Table S1, the most medium-length umami peptide DWDPHGL has lower T1R1 (–9.7 kcal/mol) and T1R3 (–10.2 kcal/mol) binding energy than GANQLDPR, LTPEPEH, and VPEPEPH. And for umami-enhancing peptide NVNPWHN, it has the lowest binding energy to T1R3 (–10.7 kcal/mol). However, for short peptides with stronger umami taste, the binding energy to T1R3 ranges from –9.7 to −7.9 kcal/mol, lower than medium-length peptides. This shows the advantage of docking energy in screening medium-length umami peptides, and the limitations of screening short peptides only considering one receptor binding energy.

The main forces of peptides to T1R1-T1R3 were electrostatic and van der Waals, induced hydrogen bond and hydrophobic interactions. For T1R1, the peptides DWDPHGL, GANQLDPR, LTPEPEH, VPEPEPH, FREE, LDFR, QEGW, and RDH formed 5, 11, 8, 9, 5, 3, 5, and 6 hydrogen bonds, respectively, much lower than hydrophobic interactions numbers 112, 130, 96, 112, 59, 56, 61, and 64. From the heatmap result, hydrogen bonds accounted for only 4.27–8.57% of total contact bond numbers. This process involved frequent contact residues ASP147, SER148, ARG151, TYR220, SER276, and ALA302. Among them, the residues SER148, TYR220, and ALA302 that formed hydrogen bonds were consistent with the molecular dynamics simulation result of umami peptide KGDEESLA with receptor T1R1 (Liu et al., 2019). These residues, have also been reported to play important roles in the interaction of T1R1 with *Oncorhynchus mykiss* umami peptides EANK, EEAK, and EMQK (Zhao et al., 2023). Therefore, the key residues between umami peptide and T1R1 may not be affected by peptide length.

For T1R3, the above eight peptides formed 8, 11, 7, 6, 5, 5, 5 and 9 hydrogen bonds, respectively. Similar to T1R1 conditions, hydrophobic interaction bonds were much larger, with sums of 79, 101, 87, 92, 76, 88, 88, and 64 respectively. Hydrogen bonds account for 5.37–12.32% of total contact numbers, which are more than T1R1 conditions. From the heatmap results, the most related residues were HIS145, SER146, TYR218, SER276, and ALA302. In the T1R3 interaction of Atlantic cod-derived umami peptides INKPGL, GPDPER, and PSPAPR, residues HIS145, SER146, TYR218, and ALA302 were shown to be key residues by CDOCKER docking (Zhu et al., 2021). The residues SER146, SER276, and ALA302 were also found in T1R3-binding long-chain mandarin fish umami peptides (Yang et al., 2022a), a study that used a different protein template (PDB: 1EWK) and CDOCKER software for T1R3 modeling and docking. In addition, the results also showed that SER residues frequently occur in umami peptide interaction with T1R1-T1R3, in line with results in chicken breast soup (Zhang et al., 2023b).

The above results revealed that the key residues were conserved for umami peptide binding to the T1R1-T1R3 domain, although the process may be affected by the quality of the receptor model, the computational molecular force field, the size of the docking region, and the length of the target peptide. Moreover, hydrophobic contact always maintains a dominant role in the binding process. Overall, the above analysis provides some basic insight into Huangjiu umami peptides.

3.5. Molecular dynamics simulation of peptide-T1R1 complex

The identified medium-length peptide DWDPHGL with most umami intensity was selected as a case study to investigate the dynamics details of interaction to T1R1 receptor in a water environment. In Fig. 4A, although the RMSD values of DWDPHGL-T1R1 were larger than DWDPHGL and T1R1, they were all within 1 Å, which revealed that the backbone structure fluctuation had not changed too much, even though the binding process could decreased the stability.

After simulation for 80 ns, the constant RMSD values indicated that the constructed system reached equilibrium. Conversely, the intermolecular hydrogen bond between DWDPHGL and T1R1 also becomes stable and mostly within 4–12 (Fig. 4B). During simulation, the flexible peptide changes its geometrical position to remain on the receptor T1R1 pocket, and tends to the path of the lowest potential energy surface. At the equilibrium stage (80–100 ns), the DWDPHGL-T1R1 complex remains stable, and a group of blue energy basin areas in the free energy landscape (FEL) results suggests that there was only one lowest energy configuration formed (Fig. 4C). The FEL map was generated based on the RMSD and radius of gyration with a series of gmx tools, such as covar, anaeig and sham. Subsequently, the energy decomposition of DWDPHGL-T1R1 showed that van der Waals and electrostatic force contributed mostly to binding, and the total energy was −40.62 kcal/

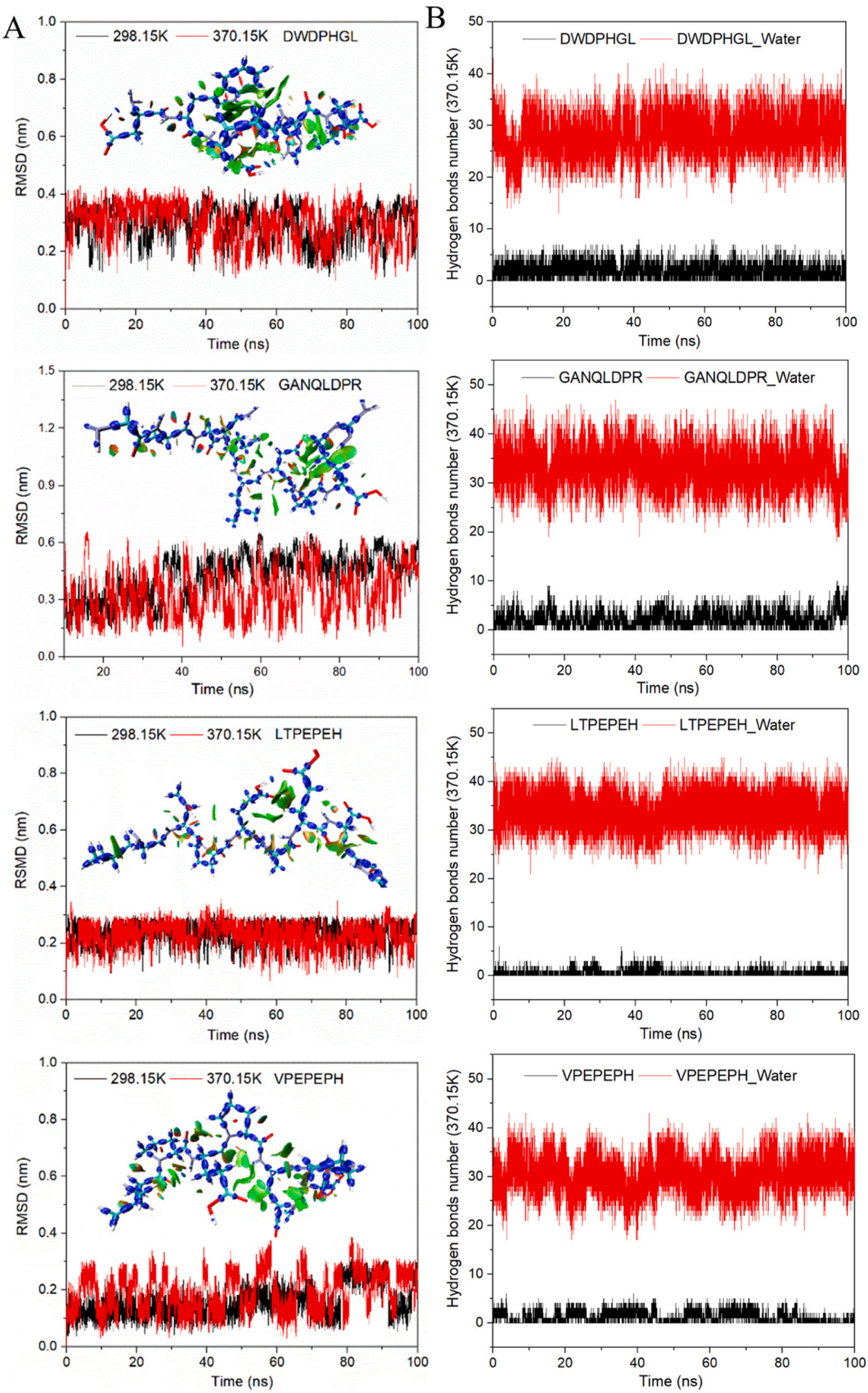

Fig. 5. The intramolecular forces analysis of four verified medium-length umami peptides (Fig. A, B represent RMSD values and hydrogen bonds counts of peptides DWDPHGL, GANQLDPR, LTPEPEH, and VPEPEPH, respectively).

mol (Fig. 4D). The Lennard-Jones short range potential results also demonstrated this process (Fig. 4E). For visualization averaged covalent and non-covalent interactions between DWDPHGL and T1R1 in trajectory frames, the aIGM calculation was also performed. The aIGM method was derived from the independent gradient model (IGM) theory, which is based on electron density. The aIGM results in Fig. 4F showed that the residues HIS71, ARG277, GLN278, ARG281, ARG307, SER382, SER384, and SER385 were mainly involved in the dynamic binding process. The green and blue isosurfaces represent the van der Waals force and hydrogen bond interaction, respectively. These residues were consistent with the result of dynamic binding of umami peptide DGF (Song et al., 2023) and KGDEESLA (Liu et al., 2019) to T1R1.

3.6. The thermal stability mechanism of the umami peptides

Stability of flavor peptide processing is critical to maintaining the function and structure–activity relationship, especially medium-length peptides (Alim et al., 2019; Liao et al., 2020). All umami peptides exhibited certain thermal stability at water according to sensory evaluation, but the relevant mechanism still needs to be explored. Molecular dynamics simulation is a powerful and intuitive tool for visualizing molecular motion processes. As shown in Fig. 5A, all RMSD values were in the range of 0.2–0.6 Å, and the peptide motion at 373.15 K became more flexible due to the larger RMSD values than 298.15 K. Although heating affected peptide stability, but the peptide backbone fluctuation did not change dramatically, because RMSD values remained within 1 Å during the 100 ns simulation period. The reason may be linked to the abundant weak molecular interactions between the water and the peptides or the peptide itself. From the IRI analysis, results revealed that four peptides were abundant with C–C covalent bonds (dark blue) and Van der Waals interactions (green). It was noted that the isosurface distribution of intramolecular interaction forces in four peptides, including Van der Waals and electrostatic, was related to the number of internal hydrogen bond peptides themselves, as shown in Fig. 5B. The isosurfaces of DWDPHGL and GANQLDPR were both more than VPEPEPH and LTPEPEH, corresponding to intramolecular hydrogen bond count numbers. On the other hand, the intermolecular hydrogen bond results (Fig. 5B) of four peptides during simulation showed that the water molecular shell surrounded by peptides formed significantly more counts than peptides themselves. These abundant hydrogen-bond networks may be a reason to keep the peptide conformation stable. Therefore, the weak interactions, particularly the intramolecular Van der Waals forces and intermolecular hydrogen bond contributed considerably to the thermal stability of the umami peptides.

4. Conclusion

In this study, a total of 1901 Huangjiu potential umami peptides were identified from the most umami fraction by peptidomics with nano-HPLC–MS/MS. The in silico screening methods and sensory evaluation verified eight novel peptides exhibited umami and thermal stability, most of them also had umami enhancement effect. In addition, RDH with DoT factor of 1.12 may be one of the key umami peptides in Huangjiu. Molecular docking revealed that peptides bind with T1R1-T1R3 key active residues to form stable complexes through hydrogen bonds and hydrophobic forces. Moreover, molecular dynamics simulation and IRI analysis proved that the intramolecular forces of medium-length peptides was very necessary to thermal stability. Considering the important flavor and health role of peptides in fermented wines, the present study could serve as a reference for other fermented wines.

CRediT authorship contribution statement

Rui Chang: Writing – original draft, Data curation, Conceptualization, Methodology, Formal analysis. **Zhilei Zhou:** Writing – review & editing, Conceptualization, Supervision, Validation. **Yong Dong:** Data curation, Validation. **Yue zheng Xu:** Resources, Supervision. Supervision. **Zhongwei Ji:** Supervision. **Shuangping Liu:** Supervision. **Jian Mao:Min Gong:** Funding acquisition, Resources, Supervision.

Declaration of Competing Interest

The authors declare that they have no known competing financial interests or personal relationships that could have appeared to influence the work reported in this paper.

Data availability

Data will be made available on request.

Acknowledgments

This research was funded by National Key Research and Development Program of China (No. 2022YFD2101204) and National Natural Science Foundation of China (22138004 and 32001828).

Appendix A. Supporting information

Supplementary data associated with this article can be found in the online version at doi:10.1016/j.jfca.2023.105822.

References

Alim, A., Yang, C., Song, H., Liu, Y., Zou, T., Zhang, Y., Zhang, S., 2019. The behavior of umami components in thermally treated yeast extract. Food Res. Int. 120, 534–543.
Chang, J., Li, X., Liang, Y., Feng, T., Sun, M., Song, S., Yao, L., Wang, H., Hou, F., 2023. Novel umami peptide from Hypsizygus marmoreus hydrolysate and molecular docking to the taste receptor T1R1/T1R3. Food Chem. 401, 134163.
Charoenkwan, P., Nantasenamat, C., Hasan, M.M., Moni, M.A., Manavalan, B., Shoombuatong, W., 2021. UMPred-FRL: A new approach for accurate prediction of umami peptides using feature representation learning. Int. J. Mol. Sci. 22 (23), 13124.
Chen, M., Gao, X., Pan, D., Xu, S., Zhang, H., Sun, Y., He, J., Dang, Y., 2021. Taste characteristics and umami mechanism of novel umami peptides and umami-enhancing peptides isolated from the hydrolysates of Sanhuang Chicken. Eur. Food Res. Technol. 247 (7), 1633–1644.
Cui, Z., Zhang, Z., Zhou, T., Zhou, X., Zhang, Y., Meng, H., Wang, W., Liu, Y., 2023. A TastePeptides-Meta system including an umami/bitter classification model Umami_YYDS, a TastePeptidesDB database and an open-source package Auto_Taste_ML. Food Chem. 405, 134812.
Dang, Y., Gao, X., Ma, F., Wu, X., 2015. Comparison of umami taste peptides in water-soluble extractions of Jinhua and Parma hams. LWT Food Sci. Technol. 60 (2), 1179–1186.
Dang, Y., Gao, X., Xie, A., Wu, X., Ma, F., 2014. Interaction between umami peptide and taste receptor T1R1/T1R3. Cell Biochem. Biophys. 70 (3), 1841–1848.
Desportes, C., Charpentier, M., Duteurtre, B., Maujean, A., Duchiron, F., 2001. Isolation, identification, and organoleptic characterization of low-molecular-weight peptides from white wine. Am. J. Enol. Vitic. 52 (4), 376–380.
Han, F.L., Xu, Y., 2011. Identification of low molecular weight peptides in Chinese rice wine (Huang Jiu) by UPLC-ESI-MS/MS. J. Inst. Brew. 117 (2), 238–250.
Kim, M.J., Son, H.J., Kim, Y., Misaka, T., Rhyu, M.-R., 2015. Umami–bitter interactions: the suppression of bitterness by umami peptides via human bitter taste receptor. Biochem. Biophys. Res. Commun. 456 (2), 586–590.
Kiyono, T., Hirooka, K., Yamamoto, Y., Kuniishi, S., Ohtsuka, M., Kimura, S., Park, E.Y., Nakamura, Y., Sato, K., 2013. Identification of pyroglutamyl peptides in Japanese rice wine (sake): presence of hepatoprotective pyroGlu-Leu. J. Agric. Food Chem. 61 (47), 11660–11667.
Li, C., Hua, Y., Pan, D., Qi, L., Xiao, C., Xiong, Y., Lu, W., Dang, Y., Gao, X., Zhao, Y., 2023. A rapid selection strategy for umami peptide screening based on machine learning and molecular docking. Food Chem. 404, 134562.
Li, X., Xie, X., Wang, J., Xu, Y., Yi, S., Zhu, W., Mi, H., Li, T., Li, J., 2020. Identification, taste characteristics and molecular docking study of novel umami peptides derived from the aqueous extract of the clam Meretrix meretrix Linnaeus. Food Chem. 312, 126053.
Liang, L., Zhou, C., Zhang, J., Huang, Y., Zhao, J., Sun, B., Zhang, Y., 2022. Characteristics of umami peptides identified from porcine bone soup and molecular docking to the taste receptor T1R1/T1R3. Food Chem. 387, 132870.
Liao, Y., Wang, W., Chen, G., Zhang, N., Liu, Y., 2020. Basic taste characteristics of flavor material from cultured Takifugu obscurus by-products. Flavour Fragr. J. 35 (3), 320–328.
Liu, H., Da, L.-T., Liu, Y., 2019. Understanding the molecular mechanism of umami recognition by T1R1-T1R3 using molecular dynamics simulations. Biochem. Biophys. Res. Commun. 514 (3), 967–973.

Liu, Z., Zhu, Y., Wang, W., Zhou, X., Chen, G., Liu, Y., 2020. Seven novel umami peptides from Takifugu rubripes and their taste characteristics. Food Chem. 330, 127204.
Lu, T., Chen, F., 2012. Multiwfn: A multifunctional wavefunction analyzer. J. Comput. Chem. 33 (5), 580–592.
Lu, T., Chen, Q., 2021. Interaction region indicator: a simple real space function clearly revealing both chemical bonds and weak interactions. Chemistry-Methods 1 (5), 231–239.
Lu, T., Chen, Q., 2023. Visualization Analysis of Weak Interactions in Chemical Systems.
Minkiewicz, P., Iwaniak, A., Darewicz, M., 2019. BIOPEP-UWM database of bioactive peptides: Current opportunities. Int. J. Mol. Sci. 20 (23), 5978.
Shen, F., Niu, X., Yang, D., Ying, Y., Li, B., Zhu, G., Wu, J., 2010. Determination of amino acids in Chinese rice wine by Fourier transform near-infrared spectroscopy. J. Agric. Food Chem. 58 (17), 9809–9816.
Shi, Y., Feng, R., Mao, J., Liu, S., Zhou, Z., Ji, Z., Chen, S., Mao, J., 2021. Structural characterization of peptides from huangjiu and their regulation of hepatic steatosis and gut microbiota dysbiosis in hyperlipidemia mice. Front. Pharmacol. 12, 689092.
Song, S., Zhuang, J., Ma, C., Feng, T., Yao, L., Ho, C.-T., Sun, M., 2023. Identification of novel umami peptides from Boletus edulis and its mechanism via sensory analysis and molecular simulation approaches. Food Chem. 398, 133835.
Spaggiari, G., Di Pizio, A., Cozzini, P., 2020. Sweet, umami and bitter taste receptors: state of the art of in silico molecular modeling approaches. Trends Food Sci. Technol. 96, 21–29.
Wang, W., Cui, Z., Ning, M., Zhou, T., Liu, Y., 2022. In-silico investigation of umami peptides with receptor T1R1/T1R3 for the discovering potential targets: a combined modeling approach. Biomaterials 281, 121338.
Wen, L., Bi, H., Zhou, X., Jiang, Y., Zhu, H., Fu, X., Yang, B., 2022. Structure characterization of soybean peptides and their protective activity against intestinal inflammation. Food Chem. 387, 132868.
Xie, G.F., Yang, D.D., Liu, X.Q., Cheng, X.X., Rui, H.F., Zhou, H.J., 2016. Correlation between the amino acid content in rice wine and protein content in glutinous rice. J. Inst. Brew. 122 (1), 162–167.
Xiong, Y., Gao, X., Pan, D., Zhang, T., Qi, L., Wang, N., Zhao, Y., Dang, Y., 2022. A strategy for screening novel umami dipeptides based on common feature pharmacophore and molecular docking. Biomaterials 288, 121697.
Yamasaki, Y., Maekawa, K., 1978. A peptide with delicious taste. Agric. Biol. Chem. 42 (9), 1761–1765.
Yang, D., Li, C., Li, L., Chen, S., Hu, X., Xiang, H., 2022a. Taste mechanism of umami peptides from Chinese traditional fermented fish (Chouguiyu) based on molecular docking using umami receptor T1R1/T1R3. Food Chem. 389, 133019.
Yang, Y., Zhou, Z., Liu, Y., Xu, X., Xu, Y., Zhou, W., Chen, S., Mao, J., 2022b. Non-alcoholic components in huangjiu as potential factors regulating the intestinal barrier and gut microbiota in mouse model of alcoholic liver injury. Foods 11 (11), 1537.
Zan, R., Wu, Q., Chen, Y., Wu, G., Zhang, H., Zhu, L., 2023. Identification of novel dipeptidyl peptidase-IV inhibitory peptides in chickpea protein hydrolysates. J. Agric. Food Chem.
Zhang, J., Zhang, J., Liang, L., Sun, B., Zhang, Y., 2023a. Identification and virtual screening of novel umami peptides from chicken soup by molecular docking. Food Chem. 404, 134414.
Zhang, L., Pu, D., Zhang, J., Hao, Z., Zhao, X., Sun, B., Zhang, Y., 2023b. Identification of novel umami peptides in chicken breast soup through a sensory-guided approach and molecular docking to the T1R1/T1R3 taste receptor. J. Agric. Food Chem.
Zhang, L., Sun, X., Lu, X., Wei, S., Sun, Q., Jin, L., Song, G., You, J., Li, F., 2022. Characterization of peanut protein hydrolysate and structural identification of umami-enhancing peptides. Molecules 27 (9), 2853.
Zhang, Y., Gao, X., Pan, D., Zhang, Z., Zhou, T., Dang, Y., 2021. Isolation, characterization and molecular docking of novel umami and umami-enhancing peptides from Ruditapes philippinarum. Food Chem. 343, 128522.
Zhao, J., Liao, S., Bi, X., Zhao, J., Liu, P., Ding, W., Che, Z., Wang, Q., Lin, H., 2022. Isolation, identification and characterization of taste peptides from fermented broad bean paste. Food Funct. 13 (16), 8730–8740.
Zhao, W., Su, L., Huo, S., Yu, Z., Li, J., Liu, J., 2023. Virtual screening, molecular docking and identification of umami peptides derived from Oncorhynchus mykiss. Food Sci. Hum. Wellness 12 (1), 89–93.
Zhou, M., Bu, T., Zheng, J., Liu, L., Yu, S., Li, S., Wu, J., 2021. Peptides in brewed wines: formation, structure, and function. J. Agric. Food Chem. 69 (9), 2647–2657.
Zhu, W., He, W., Wang, F., Bu, Y., Li, X., Li, J., 2021. Prediction, molecular docking and identification of novel umami hexapeptides derived from Atlantic cod (Gadus morhua). Int. J. Food Sci. Technol. 56 (1), 402–412.
Zhuang, M., Zhao, M., Lin, L., Dong, Y., Chen, H., Feng, M., Sun-Waterhouse, D., Su, G., 2016. Macroporous resin purification of peptides with umami taste from soy sauce. Food Chem. 190, 338–344.